MCTR1 alleviates lipopolysaccharide-induced acute lung injury by protecting lung endothelial glycocalyx

Li, Hui; Hao, Yu; Yang, Li Li; Wang, Xin Yang; Li, Xin Yu; Bhandari, Suwas; Han, Jun; Liu, Yong Jian; Gong, Yu Qiang; Scott, Aaron; Smith, Fang Gao; Jin, Sheng Wei

DOI:
10.1002/jcp.29628
10.1002/jcp.29628

Title Page

MCTR1 Alleviates Lipopolysaccharide-Induced Acute Lung Injury by Protecting Lung Endothelial Glycocalyx

Hui Li[1,2#]; Yu Hao[1#]; Li-Li Yang[1#]; Xin-Yang Wang[1]; Xin-Yu Li[1]; Suwas Bhandari[1]; Jun Han[1]; Yong-Jian Liu[1]; Yu-Qiang Gong[1]; Aaron Scott[3]; Fang Gao Smith[1, 3, 4&]; Sheng-Wei Jin[1&]

[1]Department of Anaesthesia and Critical Care, The Second Affiliated Hospital and Yuying Children's Hospital of Wenzhou Medical University, Zhejiang, China

[2]Key Laboratory of Anaesthesiology of Zhejiang Province, The Second Affiliated Hospital and Yuying Children's Hospital of Wenzhou Medical University, Zhejiang, China

[3]The Birmingham Acute Care Research (BACR) group, Institute of Inflammation and Ageing, University of Birmingham, U.K.

[4]Academic Department of Anaesthesia, Critical Care, Pain and Resuscitation, Birmingham Heartlands Hospital, Heart of England National Health Service Foundation Trust, Birmingham B9 5SS, United Kingdom

[5]This work was funded by the grants from the National Natural Science Foundation of China (No. 81870065), the Natural Science Foundation of Zhejiang Province (No.

LY19H150002, No. LQ20H150003) and the Wenzhou Science and Technology Bureau Project (No. Y20190087, No. Y20190118)

[5]The authors have no financial conflicts of interests.

[#]Three authors contribute to this work equally.

[&]Correspondence:

Sheng-Wei Jin, E-mail: jinshengwei69@163.com

Fang Gao Smith, E-mail: f.gaosmith@bham.ac.uk

Address: Department of Anaesthesia and Critical Care, Second Affiliated Hospital and Yuying Children's Hospital of Wenzhou Medical University, 109 Xueyuan Road, Wenzhou, Zhejiang Province, P. R. China 325027.

Telephone: 0086-577-88002806 Fax number: 0577-88832693

Running title: MCTR1 Alleviates Acute Lung Injury

Total number of words: 6082

ABSTRACT

Endothelial glycocalyx degradation, critical for increased pulmonary vascular permeability, is thought to facilitate the development of sepsis into the multiple organ failure. Maresin conjugates in tissue regeneration1 (MCTR1), a macrophage-derived lipid mediator, exhibits potentially beneficial effects via the regulation of bacterial phagocytosis, promotion of inflammation resolution and regeneration of tissue. In this study, we show that MCTR1 (100 ng/mouse) enhances the survival of mice with LPS-induced (15 mg/kg) sepsis. MCTR1 alleviates LPS (10 mg/kg)-induced lung dysfunction and lung tissue inflammatory response, decreasing inflammatory cytokines (TNF-α, IL-1β and IL-6) expression in serum and reducing the serum levels of heparan sulfate (HS) and syndecan-1 (SDC-1). In HUVEC experiments, MCTR1 (100 nM) was added to the culture medium with LPS for 6 h. MCTR1 treatment markedly inhibited HS degradation by downregulating heparanase (HPA) protein expression in vivo and in vitro. Further analyses indicated that MCTR1 upregulates sirtuin 1 (SIRT1) expression and decreases NF-κB p65 phosphorylation. In the presence of BOC-2 or EX527, the above effects of MCTR1 were abolished. These results suggest that MCTR1 protects against LPS-induced sepsis in mice by attenuating pulmonary endothelial glycocalyx injury via the ALX/SIRT1/NF-κB/HPA pathway.

KEYWORDS

MCTR1, sepsis, endothelial glycocalyx, HPA, SIRT1

INTRODUCTION

Sepsis is a frequent and severe medical syndrome characterized by a systemic inflammatory response and organ dysfunction to infection(Englert, Bobba, & Baron, 2019). Acute respiratory distress syndrome (ARDS) is a severe complication of sepsis characterized by pulmonary-vascular-hyperpermeability(Prescott & Angus, 2018). Excess fluid leaks out of the lung capillaries and fills the adjacent alveolar spaces causing pulmonary edema. This fluid impairs gas exchange across the alveolar membrane, decreases respiratory compliance and severely compromises lung function(Matthay, Ware, & Zimmerman, 2012). Therapies to prevent or treat lung injury in sepsis remain elusive(Leaf & Waikar, 2014; Matthay, McAuley, & Ware, 2017); therefore, it is vital to alleviate lung endothelial barrier dysfunction to resolve sepsis-induced ARDS.

The endothelial glycocalyx forming a vast endothelial surface layer (ESL) is a gel-like layer lining the luminal surface of endothelial cells(Uchimido, Schmidt, & Shapiro, 2019). It is composed of a network of proteoglycans, predominantly transmembrane bound syndecan-1 (SDC-1) and membrane-bound glycosaminoglycans (GAGs), including heparan sulfate (HS), chondroitin sulfate (CS), and hyaluronic acid (HA)(Uchimido et al., 2019). HS represents the most common ESL GAG, with HS proteoglycans accounting for 50-90% of endothelium-associated proteoglycans. The endothelial glycocalyx performs several critical functions relevant to vascular

homeostasis(LaRiviere & Schmidt, 2018; Schmidt et al., 2012). The ESL forms a fiber mesh overlaying cell-cell junctions and serves as a barrier, especially in the lungs, with particularly high concentrations of HS to oppose fluid flux out of the vascular lumen. Accordingly, the enzymatic degradation of HS and HS-associated proteoglycans from isolated perfused vessels may increase vascular permeability(Yang & Schmidt, 2013). The ESL also inhibits microvascular thrombosis and helps regulate leukocyte adhesion to the endothelium. Animal and human studies have demonstrated that ESL degradation plays a pathogenic role in the onset of vascular injury during sepsis. The sepsis-associated induction of heparanase (HPA) triggers the degradation of vascular HS, which collapses the pulmonary ESL and contributes to pulmonary injury by promoting pulmonary edema and neutrophil adhesion(Chelazzi, Villa, Mancinelli, De Gaudio, & Adembri, 2015). Therefore, the development of new therapeutic agents to alleviate glycocalyx damage and enhance glycocalyx restoration has become a necessity.

Maresin conjugates are novel lipid mediators of inflammation and resolution. Maresin conjugates in tissue regeneration 1 (MCTR1) is found in inflammatory exudates from infected mice as well as in human plasma, serum and the spleen, and its expression is increased during the late stages of infectious inflammation in mice(Dalli et al., 2016). MCTR1 is produced by 14-lipoxygenation of docosahexaenoic acid (DHA) through 12-LOX-mediated pathways in macrophages. It accelerates the resolution of E. coli infections, regulates bacterial clearance, and promotes tissue repair and regeneration. A recent study demonstrated that MCTR1 (1-100 nM) functionally counters leukotriene

D4-mediated vascular responses, including vascular leakage in mouse cremaster vessels and heartbeat reduction in primordial tunicate hearts(Chiang et al., 2018). However, the effect of MCTR1 on experimental sepsis remains unknown.

In this study, we determined the effect of MCTR1 on LPS-induced sepsis in mice based on the survival rate, lung function and inflammatory response. Furthermore, we tested the impact of MCTR1 on LPS-induced ESL injury and its underlying mechanisms to gain a better understanding. Our results suggest that MCTR1 is an endothelial glycocalyx-targeting treatment strategy.

MATERIALS AND METHODS

Materials

MCTR1 was obtained from Cayman Chemical (Ann Arbor, MI). Lipopolysaccharide (LPS), dimethyl sulfoxide (DMSO) and paraformaldehyde were purchased from Sigma-Aldrich (St. Louis, MO). The kits for measuring the plasma concentrations of TNF-α, IL-6, IL-1β, HS, and SDC-1 were obtained from R&D Systems (Minneapolis, MN). A rabbit polyclonal antibody against p-p65 was purchased from Cell Signaling Technology (Beverly, MA). A mouse anti-heparan sulfate proteoglycan 2/perlecan antibody, rabbit polyclonal antibodies against HPA and NF-κB/p65, mouse polyclonal antibodies against SIRT1 and HSPG2 and a donkey antibody against mouse IgG (H+L: Alexa Fluor® 594) were purchased from Abcam (Cambridge, MA). Mouse polyclonal

antibodies against β-actin were purchased from ZSGB-BIO (Shanghai, China). Peroxidase-conjugated goat antibodies against rabbit or mouse IgG (H+L) were purchased from BOYUN (Shanghai, China). Selisistat (EX527), an inhibitor of SIRT1 enzymatic activity, was purchased from MedChem Express (Shanghai, China). BOC-2 (ALX inhibitor) was obtained from Biomol-Enzo Life Sciences (Farmingdale, NY).

Animals and experimental groups

Specific pathogen-free (SPF) adult male C57BL/6 mice weighing 20-25 g were obtained from SLAC Laboratory Animal (Shanghai, China). The mice were housed in an SPF lab on a day-night cycle under controlled temperature and humidity conditions. The mice had free access to food and water, and all the procedures conducted followed the Guide for the Care and Use of Laboratory Animals. The Animal Studies Ethics Committee of Wenzhou Medical University approved the study.

The mice were administered LPS (15 mg/kg, IP) and MCTR1 (100 ng/mouse, IP) for survival experiments. The mortality of each group (n=8) was recorded twice a day up to 96 h after LPS administration. For other experiments, the mice were randomized into four groups (n=8): control group, LPS group, LPS+MCTR1 group and MCTR1 group. The mice were intraperitoneally injected with 10 mg/kg LPS and/or 100 ng MCTR1 per mouse. The mice in the control group were injected with an equivalent volume of normal saline (NS). All mice were anesthetized with 1% pentobarbital and sacrificed 6

h later. Blood was collected from the ophthalmic artery of the surviving mice, and lung samples were extracted.

Cell culture and experimental groups

Human umbilical vein endothelial cells (HUVECs) were from SGST (China). The cells were grown in an adherent manner in 25 cm2 flasks containing DMEM and fetal bovine serum (FBS) purchased from Gibco. The cells were cultured at 37°C in a 5% CO2 incubator.

Equal concentrations of HUVECs were added to the wells of six-well plates and allowed to adhere. They were further divided into five groups: control, LPS, LPS+MCTR1, LPS+MCTR1 + EX527 and LPS+MCTR1 + DMSO. The control group was left untreated, whereas the LPS and LPS+MCTR1 groups were treated with LPS (1 μg/ml). MCTR1 (100 nM) was added to the MCTR1 group cells. After being inoculated with both LPS and MCTR1, the mice were observed and monitored for 6 h. EX527 and the solvent control DMSO were added to LPS and MCTR1 before administration. The cells were incubated with EX527 (10 μM) for 24 h to ensure that the SIRT1 enzymatic activity was fully inhibited. Cover glass was placed at the bottom of the wells for cell adhesion and convenient microscopic observation by immunofluorescence.

Invasive assessment of respiratory mechanics

The Lung function test was performed as previously described(Li et al., 2017). Briefly, mice were anesthetized with 90 mg/kg pentobarbital sodium at 6 h after LPS administration and then tracheotomized. Vecuronium bromide was injected intravenously via the tail and then the mice were mechanically ventilated with a computer-controlled small-animal ventilator. Measurements of the respiratory system mechanics were assessed using a flexiVent system (Scireq, Montreal, QC, Canada) and evaluated assuming four different models. Deep Inflation was used to calculate the resulting changes in volume under controlled pressure, and the inspiratory capacity (IC) was recorded. The pressure-volume (PV) curve was used to assess the distensibility of the respiratory system over the entire IC range. A (estimate of IC), K (shape parameter), Cst (quasistatic compliance) and area (hysteresis, area in the PV loop) were determined from the analysis of the PV curves.

Subsequently, the mice were challenged with methacholine (Mch) aerosols generated with an in-line nebulizer (5 s) and administered directly at increasing concentrations (0 = saline, 3, 9 and 27 mg/ml). To measure respiratory system resistance (Rrs) and respiratory system elastance (Ers), Snapshot-150 was used. Rn, tissue damping (G) and tissue elastance (H) were recorded with a forced oscillation maneuver. The maximum response to each methacholine dose for the above parameters was assessed. SnapShot-150 is a single compartment model that reflects overall lung resistance, elastance and compliance. Quick Prime-3 (QP-3) is a constant phase model, using forced oscillation

to separate central and peripheral airways. All data were analyzed using flexiVent software (version 7.6).

Pulmonary histopathology evaluation

After mice were anesthetized, their left lungs were removed and fixed with 4% paraformaldehyde, embedded in paraffin, sectioned, dewaxed and rehydrated with xylene and an alcohol gradient. Then, we stained the slides with hematoxylin and eosin (HE) and observed the sections under a microscope (Nikon, Japan). According to the severity of inflammatory cell infiltration and hyperemia in the lung tissue and the thickness of the alveolar wall, the degree of acute lung injury was evaluated, and the lung injury score was determined.

Lung wet weight to dry weight ratio

To quantify the magnitude of pulmonary edema, we evaluated the wet weight to dry weight (W/D) ratio of the lung. Portions of the harvested wet left lungs were weighed; then, the portions were placed in an oven for 48 h at 60°C and the dry weight was subsequently measured. The W/D ratio was then calculated.

Lung vascular permeability assay

To assess pulmonary vascular leakage, we used Evans blue dye (EBD) extravasation. Five hours after LPS inoculation, EBD (20 mg/kg, Sigma-Aldrich) was administered via the caudal vein. After the dye circulated for 30 min, the lungs were perfused with

NS (25 ml). Then, the lungs were excised and imaged. After imaging, the lungs were blotted dry, weighed, and homogenized in formamide. Following overnight extraction, the tissue fluid was centrifuged at 12,000 ×g for 10 min. The EBD concentration of the supernatant was then evaluated at 620 nm absorbance by a microplate reader.

ELISA

To assess the levels of proinflammatory factors and glycocalyx degradation products in the circulation, we used pentobarbital to anesthetize the mice in each group. After the appropriate treatment was administered, the blood was collected by the orbital sinus extraction procedure, and the serum was separated for the subsequent experiment. According to the manufacturer's instructions, the concentrations of TNF-α, IL-6, IL-1β, HS and SDC-1 in the serum were measured by R&D systems ELISA kits.

Western blot

The mice were killed after LPS treatment to compare the abundance of glycocalyx-related proteins in the lungs or HUVECs in all the groups. The lungs were extracted and frozen in liquid nitrogen. The tissues were lysed in lysis buffer (RIPA: PMSF = 1:1) by grinding and further subjected to ultrasonic cleavage. The lysate was centrifuged at 12000 ×g at 4°C for 30 min, and the supernatant was taken as the total protein of the lung tissue. To extract the total protein of treated cells, we removed the medium, washed the cells three times with phosphate-buffered saline (PBS), incubated

them in lysis buffer for 10 min, scraped the cells and collected the lysate. Then, we centrifuged the lysate for tissue protein extraction, and the supernatant contained the total cell protein. All operations were carried out in an ice bath. The protein concentration was measured with a BCA kit, and we prepared it into 30 μg/10 μl aliquots with double distilled water and loading buffer. The proteins were separated by 10% SDS-PAGE at 80-120 volts in a molecular weight-dependent manner, and then the proteins were transferred to PVDF membranes. After being blocked with 10% milk in Tris-buffered saline with 0.05% Tween 20 (TBST) for 2 h, the membranes were incubated with the following primary antibodies: EXT1 (1:2000), HPA (1:1000), p65 (1:1000), p-p65 (1:1000), SIRT1 (1:1000), and β-actin (1:1000) at 4 ℃ overnight. The membranes were washed three times for 10 min per wash, incubated with an HRP-conjugated secondary antibody (1:3000) at room temperature for 1 h and washed three more times with TBST. Finally, the protein bands were visualized with electrochemiluminescence (ECL) and detected with a Bio-Rad Gel imaging system. The band intensity was analyzed with ImageJ.

Immunofluorescence

Immunofluorescence was performed with pulmonary tissues and HUVECs. The 4 μm sections of lung tissue were deparaffinized with xylene and dehydrated in a gradient series of ethanol. Furthermore, after antigen retrieval, the sections were prepared for immunofluorescence. Treated HUVECs were fixed in 4% paraformaldehyde to

continue the experiment. The tissue sections and fixed cells on cover glass were further blocked with donkey serum (Solarbio, Beijing) and incubated with an HSPG2-antibody (1:200). After being washed three times with PBS, the sections and fixed cells were incubated with a second antibody (Alexa Fluor® 594) (1:200) at 37 ℃ for 1 h and further incubated with DAPI (Abcam) for 5 min. Finally, we sealed the stained sections and cells with an antifade mounting medium (Solarbio, Beijing, China) and observed them with a fluorescence microscope (Leica).

Statistical analysis

Data are presented as the mean ± SD unless otherwise indicated; the pulmonary function parameter data are presented as the mean ± SEM to show the average values from independent experiments. Data were analyzed using Student's t-test for two-group comparisons and one-way ANOVA followed by Tukey's post hoc test for multiple comparisons. Mechanical data were evaluated using two-way ANOVA, followed by a multiple comparisons test. Kaplan-Meier analysis was used for survival and a log-rank (Mantel-Cox) test was used to assess statistical significance. GraphPad Prism 6.0 (GraphPad, San Diego, CA, USA) was used for the analyses and graphs. Results with a value of $P < 0.05$ were considered statistically significant.

RESULTS

MCTR1 restores the survival rate and lung dysfunction in septic mice

First, we evaluated the effects of MCTR1 on the LPS-induced sepsis model mice by survival curve analysis. As shown in Fig.1a, MCTR1 treatment improved the sepsis mouse survival rate significantly. Next, we performed a lung function test to determine the effects of MCTR1 on LPS-induced acute lung injury (ALI) in mice. The PV loop curve of the LPS group was lower than that of the saline group A curve. Compared with saline treatment, LPS treatment induced a statistically significant reduction in IC, Cst and A in mice, whereas MCTR1 treatment induced a significant increase. Upon the different concentration of Mch stimulation, Rrs, Ers, G and H were decreased to some extent in LPS-treated mice. These results indicate lung dysfunction in response to LPS-induced endotoxemia. MCTR1 treatment significantly reversed these changes (Fig. 1b-i). Rn and K showed little change among the three groups (shown in Supplementary Fig. a, b).

MCTR1 attenuates LPS-induced inflammatory injury in the lungs

The control group presented normal pulmonary histology. Compared to those of the control group, the lung tissues of the LPS group were markedly damaged. These tissues displayed interstitial edema, hemorrhage, and inflammatory cell infiltration, as evidenced by an increase in the lung injury scores. All other morphologic changes were not markedly increased in the LPS + MCTR1 group. There was no significant difference between the control and MCTR1 groups. MCTR1 treatment significantly reduced the LPS-induced pathologic changes, as evidenced by a decrease in the lung injury scores (Fig. 2a, b).

Next, we measured the levels of proinflammatory cytokines, including TNF-α, IL-1β and IL-6, in the serum. Relative to those in the ALI model group, the levels of inflammatory factors TNF-α, IL-1β, and IL-6 in the MCTR1-treatment group were substantially reduced (Fig. 2c-e)

MCTR1 inhibits LPS-induced endothelial glycocalyx damage in vivo

To determine the effect of MCTR1 on LPS-induced pulmonary edema, we performed a W/D weight ratio experiment. Compared with that in the control group, the W/D lung weight ratio increased significantly in the LPS group and was reduced in the LPS+MCTR1 group (Fig. 3a). The EBD assay was used to evaluate pulmonary vascular permeability in vivo. As shown in Fig. 3b and 3c, the pulmonary vascular permeability increased in the LPS group, and MCTR1 treatment reduced the lung vascular permeability in LPS-induced ALI mice.

Next, to determine the effect of MCTR1 on endothelial glycocalyx damage in LPS-induced ALI, HS in the lung tissue was tested via immunofluorescence (Fig. 3d, e). LPS decreased HS expression in the lung tissue, and MCTR1 significantly increased HS expression. After glycocalyx degradation, its degradation products, such as HS and SDC-1, enter the blood circulation, we collected the serum from mice in each group and assessed the HS and SDC-1 levels. Both HS and SDC-1 levels were markedly increased in the LPS group compared with the control group, whereas the increase was significantly attenuated in the LPS-MCTR1 group, as shown in Fig. 3f and 3g.

MCTR1 decreases HPA expression via the ALX/SIRT1/NF-κB p65 pathway in vivo

HPA is a specific endothelial glycocalyx HS-degrading enzyme. The expression of HPA in lung tissues was found to be markedly increased in the LPS group. The increased HPA expression was significantly attenuated in the LPS- MCTR1 group. Meanwhile, we found that the NF-κB p65 phosphorylation (p-p65) expression was higher in the LPS group than in the control group, and MCTR1 treatment decreased p-p65 in LPS-treated lungs. While SIRT1 expression was lower in the LPS group than in the control group, and was higher in the MCTR1 treatment group than in the LPS group (Fig. 4a). Furthermore, the protein levels of HPA and p-p65 were higher in the LPS+MCTR1+EX527 and LPS+MCTR1+BOC-2 groups than in the LPS+MCTR1 group. BOC-2(600ng/kg) and EX527(10mg/kg) markedly suppressed MCTR1-induced decreases in HPA and p-p65 protein levels (Fig. 4b).

In addition, we found the HS expression was not increased in the LPS+MCTR1+EX527 and LPS+MCTR1+BOC-2 groups compared with LPS+MCTR1 group (Fig. 4c). And the beneficial effects of MCTR1 on lung tissue histology were abrogated by treatment with EX527 and BOC-2 (Fig. 4d).

MCTR1 protects the endothelial glycocalyx in vitro

To determine the effect of MCTR1 on endothelial glycocalyx in vitro, we performed the experiment in LPS-induced HUVEC sepsis model. To identify the optimal dose and experimental time conditions, dose-response and time-course experiments were carried

out on HUVECs. The western blotting results in Supplementary Fig. c and d suggest that LPS administered at a dose of 1 μg/ml and incubated for 6 h was effective in vitro. Next, HUVECs were incubated with MCTR1 (100nM) in the presence or absence of LPS (1 μg/ml) for 6 h at 37 °C. After 6 h, as shown in Fig. 5a, LPS treatment decreased SIRT1 expression and enhanced the p-p65 in HUVECs, whereas MCTR1 treatment reversed these changes. Furthermore, as shown in Fig. 5b, the downregulation of HPA expression and p65 phosphorylation by MCTR1 was abolished by the presence of EX527 or BOC-2 in LPS-treated HUVECs. Moreover, HS levels were tested by immunofluorescence. The expression of HS in HUVECs was markedly reduced in the LPS group. The reduction in HS expression was significantly enhanced in the LPS-MCTR1 group. The MCTR1-induced increase in HS expression was absent in the presence of EX527 (Fig. 5c, d).

DISCUSSION

The present study results reveal that MCTR1 exhibits a protective effect against LPS-induced sepsis (Fig. 6). In this study, we postulate the following points:

1. MCTR1 improves the survival rate in the LPS-induced sepsis mouse model;
2. MCTR1 restores LPS-induced lung dysfunction;
3. MCTR1 alleviates the LPS-induced inflammatory response including vascular permeability, inflammatory exudation and the production of TNF-α, IL-1β and IL-6 in the lung tissues;

4. MCTR1 inhibits the loss of endothelial glycocalyx by regulating the ALX/SIRT1/NF-κB/HPA axis.

ARDS is one of the leading causes of death in sepsis. One of the most common manifestations of sepsis--induced ARDS is a decrease in lung compliance and IC(Matthay et al., 2017). Pulmonary dysfunction begins following lung infection in sepsis-induced ALI mainly due to the release of proinflammatory mediators, such as TNF-α, IL-1β, and IL-6, leading to the loss of alveolar-capillary barrier integrity, neutrophil recruitment, and alveolar edema(Prescott & Angus, 2018). In a previous study, George et al. reported that baseline resistance and compliance were not different between LPS- and PBS-exposed mice at 3 h, 6 h, and 24 h after LPS exposure(George, Chakraborty, Giembycz, & Newton, 2018). However, 3 h after LPS exposure, Mch (10-300 mg/ml) challenge induced significantly higher increases in lung resistance than PBS exposure alone. By 6 and 24 h post-LPS exposure, these effects on lung function returned to near baseline levels, and no significant differences relative to the PBS controls were apparent(Verjans et al., 2018). In this study, we demonstrated that compared with the control treatment, MCTR1 treatment improves the survival rate of septic mice. Next, we used four different ventilation modes to perform a comprehensive and systematic lung-function assessment. We found a significant decrease in IC and Cst 6 h after LPS administration in mice, which is consistent with those in the septic patients. Mch stimulation induced an increase in Rrs, suggesting airway hyperresponsiveness due to inflammation, and enhanced G and H, which reflects lung

parenchyma injury and phenotypic alterations, as well as an increased Ers, suggesting pulmonary edema. MCTR1 reversed all of the indicated changes. These results indicate that MCTR1 potentially reduces inflammation and lung edema, restoring lung function and prolonging survival.

Endothelial glycocalyx damage is among the main factors contributing to increased vascular permeability. SDC-1 and HS are the main components of the core and side-chain structures of the endothelial glycocalyx, respectively. They are often used as indicators of the integrity of the endothelial glycocalyx(Schmidt et al., 2012). Sepsis induces the heparanase-mediated degradation of the endothelial glycocalyx, which is critical for vascular homeostasis(Lerner et al., 2011). Glycocalyx fragments (e.g. HS and SDC-1) shed into the blood during sepsis may serve as clinically relevant biomarkers. It has been proven in clinical studies that a correlation between blood levels of glycocalyx components and organ dysfunction, severity, and mortality exists in sepsis(Uchimido et al., 2019). It has been also demonstrated that endothelial glycocalyx degradation in mice and HUVECs after LPS treatment(Chen et al., 2004; Sanderson, Elkin, Rapraeger, Ilan, & Vlodavsky, 2017). MCTR1 functions in tissue homeostasis and inflammation resolution. A previous study reported that MCTR1 reduces vascular leakage initiated by leukotriene D4 in mouse cremaster vessels(Chiang et al., 2018). Our present results demonstrate that MCTR1 enhances HS expression in the lung tissue, which is downregulated by LPS in vivo and vitro and decreases the serum levels of HS and SDC-1 in the LPS-induced mouse sepsis model. HPA is a well-known essential

sheddase that degrades the glycocalyx and can be activated by proinflammatory cytokines such as TNF-α, IL-1-β, IL-6 and NF-κB(Chen et al., 2004; Lerner et al., 2011; Schmidt et al., 2012). HPA inhibitors are used therapeutically for the treatment of cancer and inflammation(Sanderson et al., 2017). In this study, we found that MCTR1 treatment decreases HPA expression in vivo and in vitro.

SIRT1 has been shown to play as an anti-inflammatory role by regulating the production of proinflammatory cytokines in a CLP-induced mouse sepsis model, as well as in an LPS-induced model(Gao et al., 2015; Ong & Ramasamy, 2018; Rabadi et al., 2015). It has been reported that the activation of SIRT1 results in the inhibition of NF-κB-dependent inflammatory responses(Kauppinen, Suuronen, Ojala, Kaarniranta, & Salminen, 2013). SIRT1 deficiency promotes the activation of NF-κB(de Mingo et al., 2016; Garcia et al., 2015; Iskender et al., 2017). SIRT1 results in deacetylation and inactivation of the nuclear NF-κB p65 in vascular smooth muscle cells(Kong et al., 2019). It has been reported that NF-κB is involved in the regulation of HPA expression and further degradation of the endothelial glycocalyx in various inflammation and cancer models. NF-κB signaling activation promotes HPA expression， and the inhibition of NF-κB signaling pathway downregulating HPA expression have been found in LPS-induced ARDS(An et al., 2018; Hao et al., 2015; Huang et al., 2018; Zhang et al., 2010). Our results demonstrate that SIRT1 expression was downregulated and NF-κB p65 phosphorylation and HPA expression were upregulated in LPS-induced mice, which was reversed by MCTR1 treatment. In the presence of EX527, a SIRT1

enzymatic activity inhibitor, the effects of MCTR1 on NF-κB p65 phosphorylation, HPA and HS expression were all abolished, suggesting that SIRT1 plays a critical role in the protection against LPS-induced glycocalyx injury by MCTR1.

In conclusion, our results indicate that MCTR1 stabilizes the endothelial glycocalyx by activating SIRT1/NF-κB/HPA pathway facilitating the maintenance of the physiological endothelial barrier in response to inflammatory challenge. The preservation of the glycocalyx alleviates inflammation and tissue edema, thereby further restoring lung function and improving the endotoxemia mouse survival rate. Our findings reveal a treatment option for endotoxemia and the resolution of ARDS. The prevention of shedding promises to explain the action of MCTR1 further. However, several limitations or future works should be considered: In our study, we evaluated pulmonary ventilation function in our experimental model of indirect lung injury via lung function test. In this experimental set up however, we were unable to assay pulmonary diffusion function. As such we will attempt to evaluate arterial blood gas analysis in subsequent studies.

ACKNOWLEDGMENTS

The authors thank Hong-Xia Mei, Xiao-Ying Huang for technical assistance in our experiment. This work was funded by the grants from the National Natural Science Foundation of China (No. 81870065), the Natural Science Foundation of Zhejiang

Province (No. LY19H150002, No. LQ20H150003) and the Wenzhou Science and Technology Bureau Project (No. Y20190087, No. Y20190118).

CONFLICTS OF INTEREST

The authors have not disclosed any potential conflicts of interest.

AUTHOR CONTRIBUTIONS

H.L., Y.H., F.G.S and S.W.J made substantial contributions to the conception and design of the experiment. H.L., H.Y., L.L.Y and Y.J.L performed animal experiments; X.Y.W, X.Y.L and J.H. did cell experiments. Y.Q.G did the statistical analysis. Y.H prepared all figures. H.L., S.B and A.S wrote the main manuscript text. All authors reviewed the manuscript.

DATA AVAILABILITY

The data used to support the findings of this study are available from the corresponding author upon request.

REFERENCES

An, X., Zhang, L., Yao, Q., Li, L., Wang, B., Zhang, J., . . . Zhang, J. (2018). The receptor for advanced glycation endproducts mediates podocyte heparanase expression through NF-kappaB signaling pathway. *Mol Cell Endocrinol, 470*, 14-25. doi:10.1016/j.mce.2017.05.004

Chelazzi, C., Villa, G., Mancinelli, P., De Gaudio, A. R., & Adembri, C. (2015). Glycocalyx and sepsis-induced alterations in vascular permeability. *Crit Care, 19*, 26. doi:10.1186/s13054-015-0741-z

Chen, G., Wang, D., Vikramadithyan, R., Yagyu, H., Saxena, U., Pillarisetti, S., & Goldberg, I. J. (2004). Inflammatory cytokines and fatty acids regulate

endothelial cell heparanase expression. *Biochemistry, 43*(17), 4971-4977. doi:10.1021/bi0356552

Chiang, N., Riley, I. R., Dalli, J., Rodriguez, A. R., Spur, B. W., & Serhan, C. N. (2018). New maresin conjugates in tissue regeneration pathway counters leukotriene D4-stimulated vascular responses. *FASEB J, 32*(7), 4043-4052. doi:10.1096/fj.201701493R

Dalli, J., Vlasakov, I., Riley, I. R., Rodriguez, A. R., Spur, B. W., Petasis, N. A., . . . Serhan, C. N. (2016). Maresin conjugates in tissue regeneration biosynthesis enzymes in human macrophages. *Proc Natl Acad Sci U S A, 113*(43), 12232-12237. doi:10.1073/pnas.1607003113

de Mingo, A., de Gregorio, E., Moles, A., Tarrats, N., Tutusaus, A., Colell, A., . . . Mari, M. (2016). Cysteine cathepsins control hepatic NF-kappaB-dependent inflammation via sirtuin-1 regulation. *Cell Death Dis, 7*(11), e2464. doi:10.1038/cddis.2016.368

Englert, J. A., Bobba, C., & Baron, R. M. (2019). Integrating molecular pathogenesis and clinical translation in sepsis-induced acute respiratory distress syndrome. *JCI Insight, 4*(2). doi:10.1172/jci.insight.124061

Gao, R., Ma, Z., Hu, Y., Chen, J., Shetty, S., & Fu, J. (2015). Sirt1 restrains lung inflammasome activation in a murine model of sepsis. *Am J Physiol Lung Cell Mol Physiol, 308*(8), L847-853. doi:10.1152/ajplung.00274.2014

Garcia, J. A., Volt, H., Venegas, C., Doerrier, C., Escames, G., Lopez, L. C., & Acuna-Castroviejo, D. (2015). Disruption of the NF-kappaB/NLRP3 connection by melatonin requires retinoid-related orphan receptor-alpha and blocks the septic response in mice. *FASEB J, 29*(9), 3863-3875. doi:10.1096/fj.15-273656

George, T., Chakraborty, M., Giembycz, M. A., & Newton, R. (2018). A bronchoprotective role for Rgs2 in a murine model of lipopolysaccharide-induced airways inflammation. *Allergy Asthma Clin Immunol, 14*, 40. doi:10.1186/s13223-018-0266-5

Hao, N. B., Tang, B., Wang, G. Z., Xie, R., Hu, C. J., Wang, S. M., . . . Yang, S. M. (2015). Hepatocyte growth factor (HGF) upregulates heparanase expression via the PI3K/Akt/NF-kappaB signaling pathway for gastric cancer metastasis. *Cancer Lett, 361*(1), 57-66. doi:10.1016/j.canlet.2015.02.043

Huang, L., Zhang, X., Ma, X., Zhang, D., Li, D., Feng, J., . . . Liu, X. (2018). Berberine alleviates endothelial glycocalyx degradation and promotes glycocalyx restoration in LPS-induced ARDS. *Int Immunopharmacol, 65*, 96-107. doi:10.1016/j.intimp.2018.10.001

Iskender, H., Dokumacioglu, E., Sen, T. M., Ince, I., Kanbay, Y., & Saral, S. (2017). The effect of hesperidin and quercetin on oxidative stress, NF-kappaB and SIRT1 levels in a STZ-induced experimental diabetes model. *Biomed Pharmacother, 90*, 500-508. doi:10.1016/j.biopha.2017.03.102

Kauppinen, A., Suuronen, T., Ojala, J., Kaarniranta, K., & Salminen, A. (2013). Antagonistic crosstalk between NF-kappaB and SIRT1 in the regulation of

inflammation and metabolic disorders. *Cell Signal, 25*(10), 1939-1948. doi:10.1016/j.cellsig.2013.06.007

Kong, P., Yu, Y., Wang, L., Dou, Y. Q., Zhang, X. H., Cui, Y., . . . Han, M. (2019). circ-Sirt1 controls NF-kappaB activation via sequence-specific interaction and enhancement of SIRT1 expression by binding to miR-132/212 in vascular smooth muscle cells. *Nucleic Acids Res, 47*(7), 3580-3593. doi:10.1093/nar/gkz141

LaRiviere, W. B., & Schmidt, E. P. (2018). The Pulmonary Endothelial Glycocalyx in ARDS: A Critical Role for Heparan Sulfate. *Curr Top Membr, 82*, 33-52. doi:10.1016/bs.ctm.2018.08.005

Leaf, D. E., & Waikar, S. S. (2014). Rosuvastatin for sepsis-associated ARDS. *N Engl J Med, 371*(10), 968. doi:10.1056/NEJMc1408401

Lerner, I., Hermano, E., Zcharia, E., Rodkin, D., Bulvik, R., Doviner, V., . . . Elkin, M. (2011). Heparanase powers a chronic inflammatory circuit that promotes colitis-associated tumorigenesis in mice. *J Clin Invest, 121*(5), 1709-1721. doi:10.1172/JCI43792

Li, H., Hao, Y., Zhang, H., Ying, W., Li, D., Ge, Y., . . . Jin, S. (2017). Posttreatment with Protectin DX ameliorates bleomycin-induced pulmonary fibrosis and lung dysfunction in mice. *Sci Rep, 7*, 46754. doi:10.1038/srep46754

Matthay, M. A., McAuley, D. F., & Ware, L. B. (2017). Clinical trials in acute respiratory distress syndrome: challenges and opportunities. *Lancet Respir Med, 5*(6), 524-534. doi:10.1016/S2213-2600(17)30188-1

Matthay, M. A., Ware, L. B., & Zimmerman, G. A. (2012). The acute respiratory distress syndrome. *J Clin Invest, 122*(8), 2731-2740. doi:10.1172/JCI60331

Ong, A. L. C., & Ramasamy, T. S. (2018). Role of Sirtuin1-p53 regulatory axis in aging, cancer and cellular reprogramming. *Ageing Res Rev, 43*, 64-80. doi:10.1016/j.arr.2018.02.004

Prescott, H. C., & Angus, D. C. (2018). Enhancing Recovery From Sepsis: A Review. *JAMA, 319*(1), 62-75. doi:10.1001/jama.2017.17687

Rabadi, M. M., Xavier, S., Vasko, R., Kaur, K., Goligorksy, M. S., & Ratliff, B. B. (2015). High-mobility group box 1 is a novel deacetylation target of Sirtuin1. *Kidney Int, 87*(1), 95-108. doi:10.1038/ki.2014.217

Sanderson, R. D., Elkin, M., Rapraeger, A. C., Ilan, N., & Vlodavsky, I. (2017). Heparanase regulation of cancer, autophagy and inflammation: new mechanisms and targets for therapy. *FEBS J, 284*(1), 42-55. doi:10.1111/febs.13932

Schmidt, E. P., Yang, Y., Janssen, W. J., Gandjeva, A., Perez, M. J., Barthel, L., . . . Tuder, R. M. (2012). The pulmonary endothelial glycocalyx regulates neutrophil adhesion and lung injury during experimental sepsis. *Nat Med, 18*(8), 1217-1223. doi:10.1038/nm.2843

Uchimido, R., Schmidt, E. P., & Shapiro, N. I. (2019). The glycocalyx: a novel diagnostic and therapeutic target in sepsis. *Crit Care, 23*(1), 16. doi:10.1186/s13054-018-2292-6

Verjans, E., Kanzler, S., Ohl, K., Rieg, A. D., Ruske, N., Schippers, A., . . . Martin, C. (2018). Initiation of LPS-induced pulmonary dysfunction and its recovery occur independent of T cells. *BMC Pulm Med, 18*(1), 174. doi:10.1186/s12890-018-0741-2

Yang, Y., & Schmidt, E. P. (2013). The endothelial glycocalyx: an important regulator of the pulmonary vascular barrier. *Tissue Barriers, 1*(1). doi:10.4161/tisb.23494

Zhang, J., Chen, Y., Xin, X. L., Li, Q. N., Li, M., Lin, L. P., . . . Ding, J. (2010). Oligomannurarate sulfate blocks tumor growth by inhibiting NF-kappaB activation. *Acta Pharmacol Sin, 31*(3), 375-381. doi:10.1038/aps.2010.13

FIGURE LEGENDS

Fig. 1 MCTR1 improves the survival rate and lung function of mice after LPS administration.

Survival curves after MCTR1 (100 ng/mouse) administration in LPS (15 mg/kg)-challenged mice (**a**). Lung function was determined by the flexiVent system at 6 h after LPS (10 mg/kg) and MCTR1 (100 ng/mouse) challenge. Inspiratory Capacity (IC) (**b**), respiratory system resistance (Rrs) (**c**), respiratory system elastance (Ers) (**d**), pressure-volume loop curves (**e**), static compliance (Cst) (**f**), area (hysteresis, area in the PV loop) (**g**), G (tissue damping) (**h**), and H (tissue elastance) (**i**) are shown. Data are presented as the mean ± SEM. $^{*}P < 0.05$, $^{\#}P<0.05$ compared with the control group, $^{\&}P<0.05$ compared with the LPS+MCTR1 group, $^{\&\&}P<0.01$ compared with the LPS+MCTR1 group; n = 8 for the survival experiment, n=6 for the lung function test.

Fig. 2 MCTR1 alleviates the mouse inflammatory response after LPS administration. Mice were challenged with LPS (10 mg/kg) and MCTR1 (100

552 ng/mouse) for 6 h. Representative lung tissue sections stained with hematoxylin-eosin
553 (HE) at a magnification of 200x (**a**). Lung injury score (**b**). The inflammatory cytokines
554 TNF-α (**c**), IL-1β (**d**), and IL-6 (**e**) in the serum were measured by ELISA. Data are
555 presented as the mean ± SD. $^{**}P < 0.01$, n = 6.

556 **Fig. 3 MCTR1 inhibits LPS-induced endothelial glycocalyx damage in vivo.**
557 LPS (10 mg/kg) and MCTR1 (100 ng/mouse) were administered to mice for 6 h. Lung
558 tissue W/D weight ratio (**a**). Lung tissues from each experimental group were processed
559 for vascular permeability measurement by EBD (**b, c**). The level of HS in the lung tissue
560 was measured by immunofluorescence, scar bar=50 μm (**d, e**). After collecting serum
561 from eyeballs, and the levels of HS and SDC-1 in serum were measured by ELISA (**f,**
562 **g**). Data were presented as the mean ± SD. $^{*}P < 0.05$, $^{**}P < 0.01$, $^{***}P < 0.001$. n=6.

563 **Fig. 4 MCTR1 decreases HPA expression via the ALX/SIRT1/NF-κB pathway in**
564 **vivo.**
565 LPS (10 mg/kg) and MCTR1 (100 ng/mouse) were administered to mice for 6 h. The
566 levels of HPA, p-p65 and SIRT1 in the lung tissue were measured by western blot (**a**).
567 MCTR1(100 ng/mouse) and BOC-2(ALX receptor inhibitor, 600 ng/kg) or EX527
568 (SIRT1 inhibitor) were co-injected in mice 6 h after LPS administration. The protein
569 levels of HPA and p-p65 were measured (**b**). The level of HS in lung tissue was
570 measured by immunofluorescence, scar bar=50 μm (**c**). Representative HE-stained lung
571 tissue sections at a magnification of 200× (**d**). Data were presented as the mean ± SD.
572 $^{*}P < 0.05$, $^{**}P < 0.01$. n=6.

Fig. 5 MCTR1 inhibits HPA expression via the SIRT1/NF-κB pathway in vitro.

HUVECs were challenged with 1 μg/ml LPS and 100 nM MCTR1 for 6 h. SIRT1 and p-p65 levels were measured by western blot (**a**). In the presence of EX527 or its resolvent DMSO, the protein expressions of HPA and p-p65 were measured (**b**). The level of HS was measured by immunofluorescence, scar bar=50 μm (**c, d**). Data were presented as the mean ± SD. **P* < 0.05, ***P* < 0.01. n=6.

Fig. 6 MCTR1 protects against LPS-induced ALI in vivo and in vitro

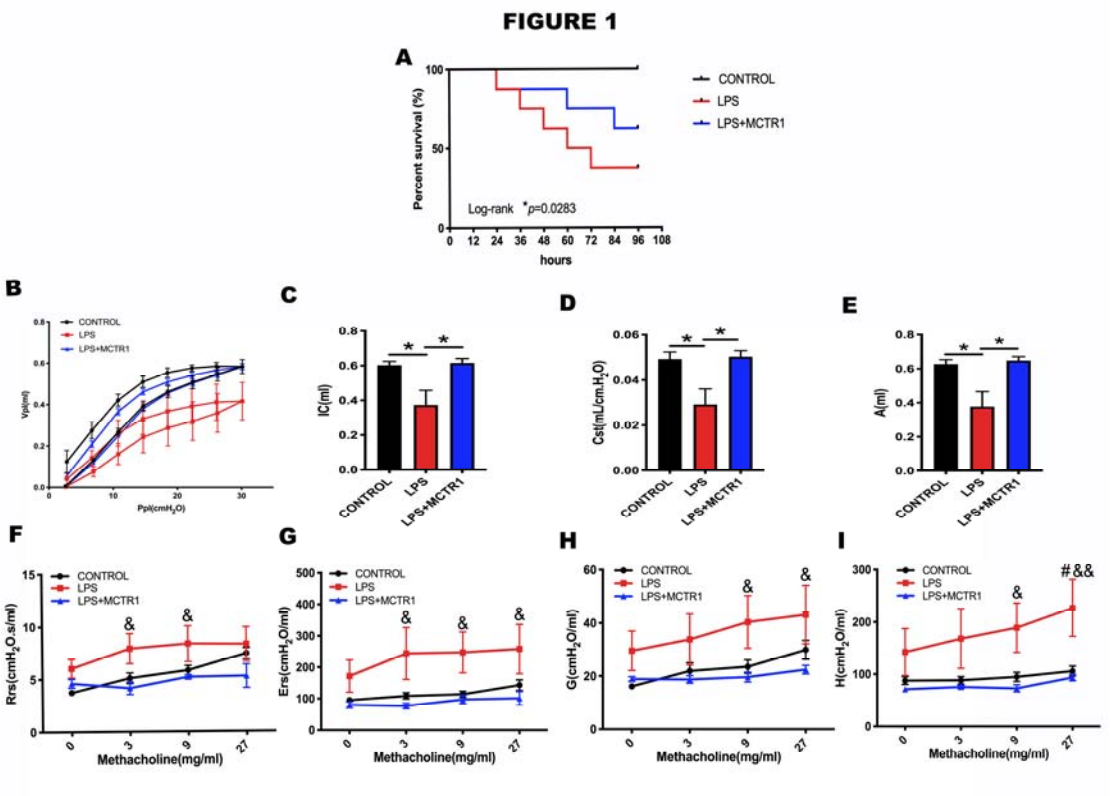

FIGURE 2

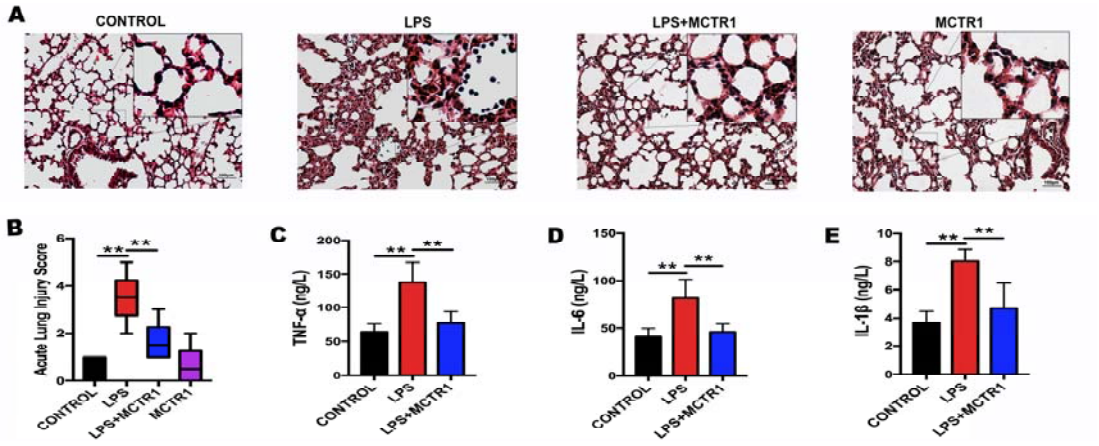

584

585

FIGURE 3

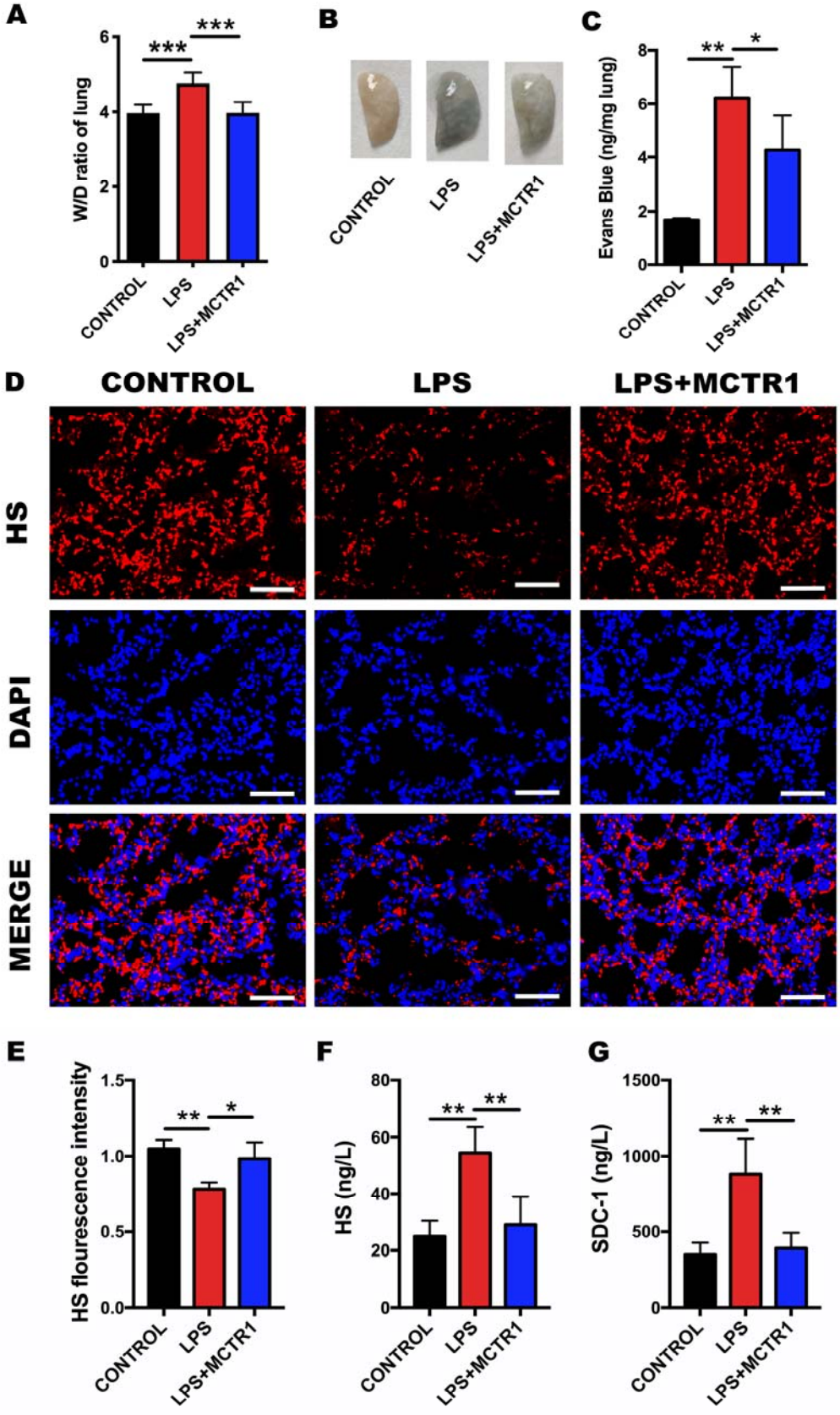

586

587

FIGURE 4

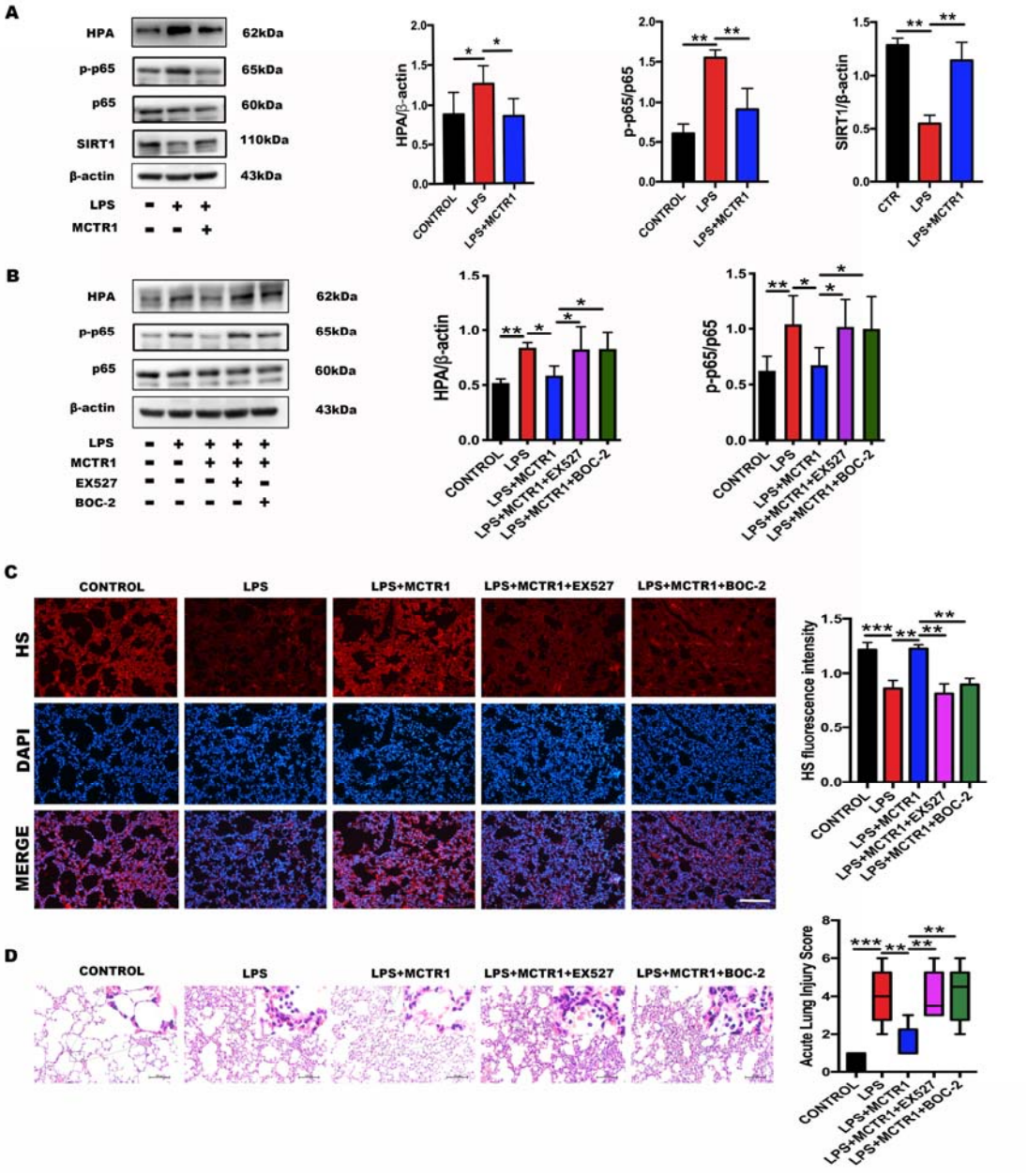

588

589

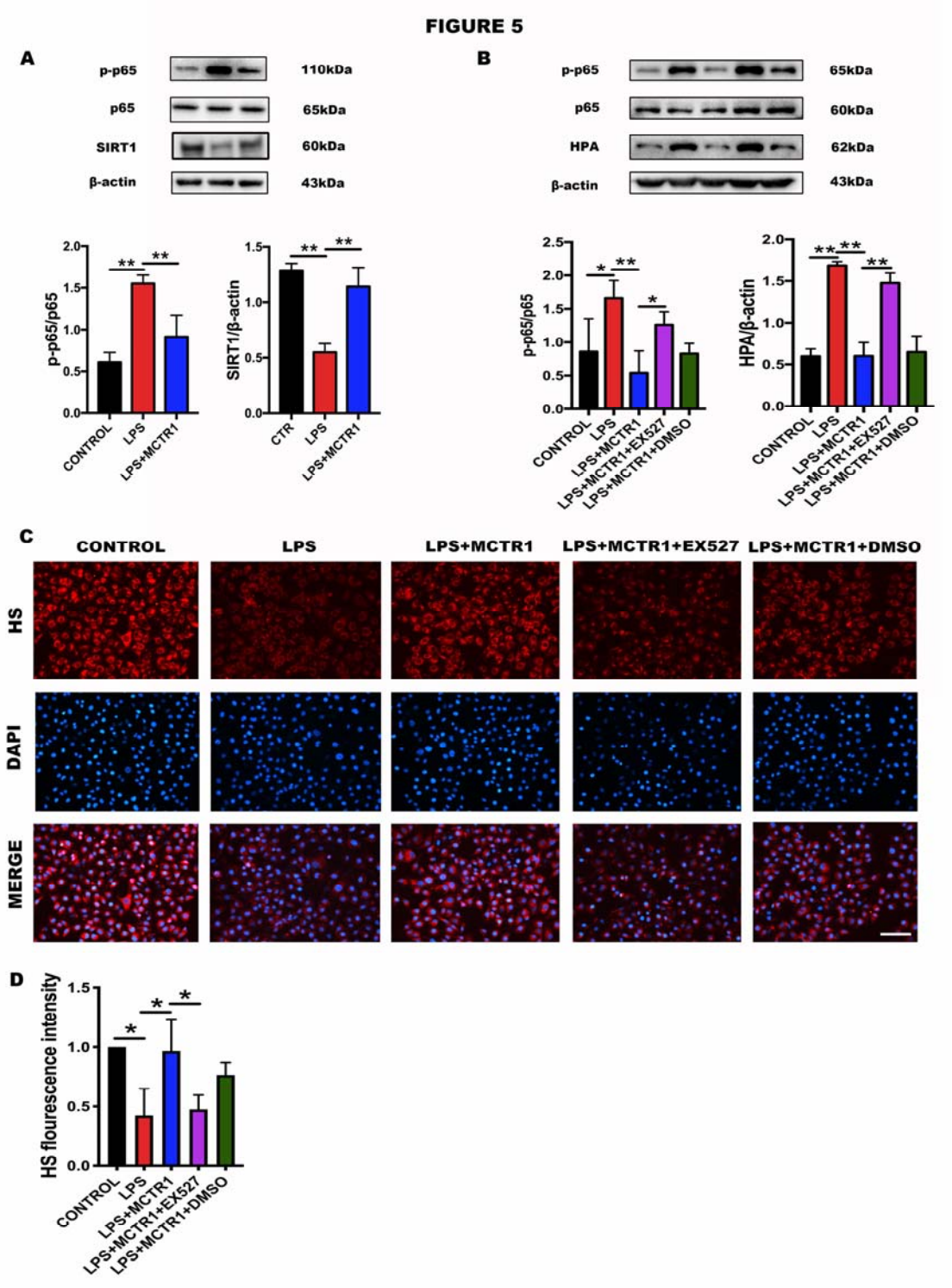
FIGURE 5
A
p-p65
p65
SIRT1
β-actin
110kDa
65kDa
60kDa
43kDa
p-p65/p65
SIRT1/β-actin
CONTROL
LPS
LPS+MCTR1
CTR
B
p-p65
p65
HPA
β-actin
65kDa
60kDa
62kDa
43kDa
p-p65/p65
HPA/β-actin
LPS+MCTR1+EX527
LPS+MCTR1+DMSO
C
CONTROL
LPS
LPS+MCTR1
LPS+MCTR1+EX527
LPS+MCTR1+DMSO
HS
DAPI
MERGE
D
HS flourescence intensity

590

591

FIGURE 6

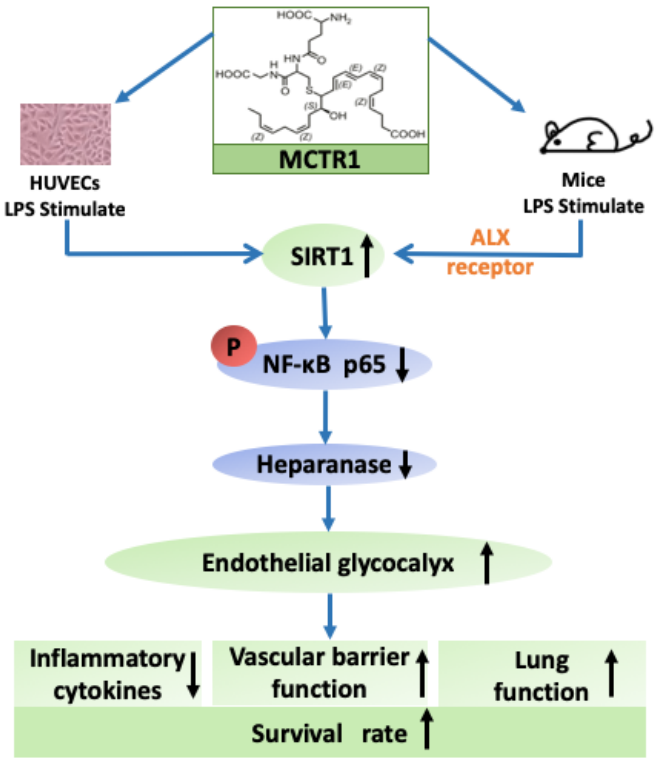
MCTR1
HUVECs
LPS Stimulate
Mice
LPS Stimulate
SIRT1
ALX
receptor
P
NF-κB p65
Heparanase
Endothelial glycocalyx
Inflammatory cytokines
Vascular barrier function
Lung function
Survival rate

592